

# Photonic irradiation induces nano-structures – an EPR study

C. FLOREA<sup>a\*</sup>, S. GEORGESCU<sup>b</sup>

<sup>a</sup>ESIEE (Ecole Supérieure d'Ingénieurs en Electronique et Electrotechnique de Paris)  
B.P. 99 – F93162 NOISY-LE-GRAND cedex France

<sup>b</sup>NILPRP (National Institute for Lasers, Plasma, and Radiation Physics)  
409 Atomistilor Street / P.O. Box MG-54 RO-77125 Romania

During the irradiation of fluorite (CaF<sub>2</sub>) with photons (X) we observe the formation of nano ordered structures (inclusions). This forming structure is homothetic in relation to the fluorine ions of the crystal. The particles of approximately 10 nm size agglomerate and form *nanostructures structures with parallelepipedic shape*. The length of these structures varies between 30 and 3000 nm. The local changes of symmetry produced by the formation of the nano structures can be inferred from EPR measurements on *Kramers rare earth ions* introduced in CaF<sub>2</sub>.

(Received March 15, 2007; accepted July 10, 2007)

**Keywords:** Nanostructures structures with parallelepipedic shape, Kramers rare earth ions, F centers, Local symmetry change, Exciton,  $\hat{G}$  tensor, Trigonal axes, Tetragonal spectrum

## 1. Introduction

A very large number of papers were devoted to the study of the changes induced in the irradiated crystals. Among the most significant, in our opinion, are the papers [1-4]. In these papers it is evidenced the role of the point defects (essentially, *F centers*) in the changes appearing as the result of the irradiation with high-energy X photons (more than 1 keV).

It seems that the F centers are produced according to the following scenario [5,6]: the incident photons ionize mainly the anionic sites. The anion ionization produces at the site a positive charge (a hole or an anionic vacancy). The vacancy traps an electron, which compensates its positive charge. The electron and the vacancy constitute a hydrogen-type object with characteristic energy levels. The resulting selective absorption is responsible for the color of the crystal (normally transparent). The assembly anionic vacancy + electron is named F center (from the German word "Farbe" for color).

To simplify, the F center can be considered as a cubic box containing an electron. The eigenvalues of the electronic energy are (if the potential vanishes inside the

box and is infinite outside): 
$$\frac{\hbar^2}{2m_0} \frac{\pi^2}{a^2} (n_x^2 + n_y^2 + n_z^2),$$

where  $\hbar$  is the rationalized Planck constant,  $m_0$  is the electron mass and  $n_x, n_y, n_z$  are non-null integer numbers. In the ground state  $n_x = n_y = n_z = 1$ , i. e. the ground state is not degenerated. The first excited state is three times degenerated: (2,1,1), (1,2,1), (1,1,2). The irradiation with photons could distort the site, and that is

equivalent with a *local symmetry change*. This distortion reduces the symmetry of the F center, removing partially the degeneracy, and diminishes the energy of the defect. The energy-configuration diagram [5] shows that the state (1,1,2) – representing an elongation or a contraction of the lattice around the F center – is predisposed to such a distortion. This spontaneous distortion of the F center (observed, also, for other defects or crystals) is of the Jahn-Teller type. Due to this effect the energy of the state is lowered, the energy being shared with two anionic neighbors, resulting an  $X_2^-$  (Fluorine, in this case) molecule oriented along  $\langle 110 \rangle$  direction.

This molecule, very electrophile, traps an electron which forms with the hole another hydrogen-like state, named *exciton*. This state is shared by two neighboring anions. The local distortion (for instance, a contraction) stabilizes this excited state denoted (1,1,2). The radiative energy of the de-excitation, diminished by the lattice distortion, could take the value zero (if the configuration-distortion curves intersect each other). In this case the energy of this non-radiative transition is completely transferred to ions. Taking into account the symmetry, the most probable event is the ejection of one of the two ions

$A^-$  in the direction of the molecule  $X_2^-$ . This direction is "dense" and formed by  $A^-$  ions of the same mass. At the time of a non-radiative de-excitation, an anion returns to its site while the other one, leaving the site, send off the nearest neighbor. The origin of this process is the photon impact; successive impacts propagate with low losses. For enough initial energy (5-8 eV), the initial ion drives off its neighbor, this one drives off its neighbor and so on. Finally,

after this series of collisions, a vacancy  $A^-$  remains in the initial position while an interstitial is present at some atomic distances where two anions share the same site. The energy of the non-radiative transition can be either found as the energy to create the two defects (vacancy 'v' and the interstitial 'i') or dissipated by the thermal agitation during collisions.

As a conclusion, we must emphasize that the creation mechanism of the nano-structures by irradiation is not yet elucidated. In order to understand better this mechanism, a series of EPR experiments on irradiated samples doped with *Kramers rare earth ions* ( $\text{Er}^{3+}$  and  $\text{Sm}^{3+}$ ), has been carried out.

## 2. Experimental

The  $\text{CaF}_2$  single crystals, doped with  $\text{Er}^{3+}$  and  $\text{Sm}^{3+}$  have been grown in the Solid State Quantum Electronics Laboratory - National Institute for Lasers, Plasma, and Radiation Physics.  $\text{Er}^{3+}$  and  $\text{Sm}^{3+}$  substitute  $\text{Ca}^{2+}$  in the  $\text{CaF}_2$  lattice. Samarium enters, also, as  $\text{Sm}^{2+}$ , with non-vanishing Van Vleck susceptibility ( $\chi_{\text{VV}}$ ). This susceptibility influences the positions and the intensities of the EPR signal of  $\text{Sm}^{3+}$ . Erbium enters only as  $\text{Er}^{3+}$ .

The  $\text{CaF}_2$  single crystals were grown in argon atmosphere. Prior to the growth, the  $\text{CaF}_2$  was purified by thermal treatments and zone melting. The doping concentrations were 1.5 % mol for Sm and 0.1 % mol for Er. Samarium was introduced as a metal while Erbium was introduced as  $\text{Er}_2\text{O}_3$ . The initial concentrations (in the non-irradiated samples) of  $\text{Sm}^{3+}$  and  $\text{Er}^{3+}$  were the same (0.05 at. % relative to  $\text{Ca}^{2+}$ ). Therefore, the intensity of  $\text{Sm}^{3+}$  EPR signal had the same order of magnitude as the  $\text{Er}^{3+}$  signal.

For crystalline structures of the fluorite type the EPR studies evidenced the role of the symmetry of the ligand field in the process of the energy transfer between the electronic energy levels. By irradiating such a crystalline structure with X-rays (~50 keV) we observe that the symmetry change of the ligand field induces the anisotropy of the  $\hat{G}$  tensor (tensor of spectral decomposition).

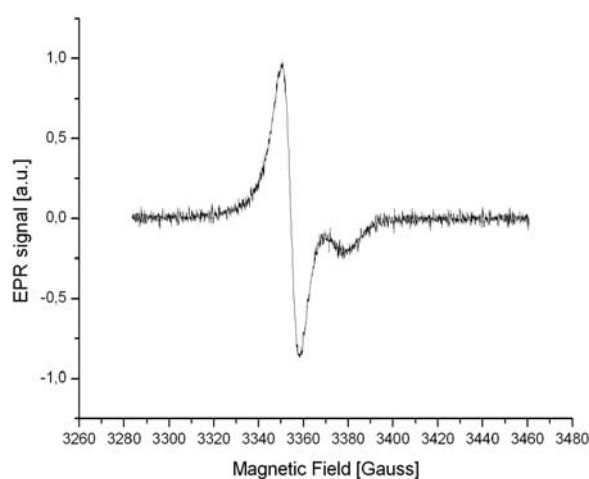
In a crystalline structure of fluorine type when the  $\text{RE}^{3+}$  (RE = rare earth) ion enters a site with cubic symmetry substituting a divalent metal ion  $\text{Me}^{2+}$ , the EPR spectra of  $\text{RE}^{3+}$  are rather complex. For  $\text{Sm}^{3+}$  it is difficult to interpret the EPR spectra in the frame of the first order of perturbation due to the small gap (~1000  $\text{cm}^{-1}$ ) between the first excited state and the ground state  $^6\text{H}_{5/2}$ . In contrast, the components  $g_{\parallel}$  and  $g_{\perp}$  of the  $\hat{G}$  tensor are well identified. In this case the gap between the first excited state  $^4\text{I}_{3/2}$  and the ground state  $^4\text{I}_{15/2}$  is large enough (~6000  $\text{cm}^{-1}$ ) and thus the first order theory of perturbations is correct.

Due to the charge compensation, the site symmetry, initially cubic, changes into longitudinal tetragonal and/or into diagonal trigonal symmetry. Nevertheless, some sites remain cubic. The new result reported in this paper is the

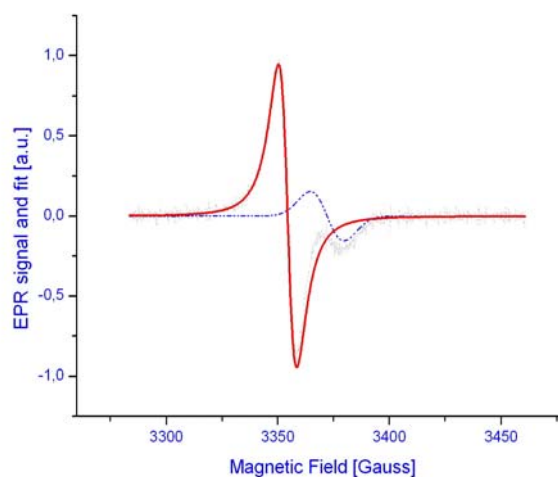
presence of an intense EPR signal characterized by a  $\hat{G}$  tensor with trigonal symmetry. This signal is very intense in the irradiated sample but it is present, with lower intensity, in non-irradiated sample.

### 2.1. EPR measurements on irradiated sample

The non-doped fluorine sample does not give any EPR signal. After the irradiation with 50 keV X photons (4 hours and, respectively, 8 hours) the EPR signals with  $g \approx 2$  are clearly observed. These EPR signals (Figs. 1 and 2) were recorded for a fixed frequency (9.4 GHz) and a variable magnetic field (3200 ÷ 3400 Gauss).



a



b

Fig. 1. a The EPR signal recorded on a  $\text{CaF}_2$  sample irradiated for 4 hours with 50 KeV X-ray photons. b The Poincaré's fit evidences the complex structure of the line: - a dominant Lorentzian contribution (~85%) due to the F centers (thick, solid line); - a minor Gaussian contribution (~15%) due to the conduction electrons (thin, dotted line).

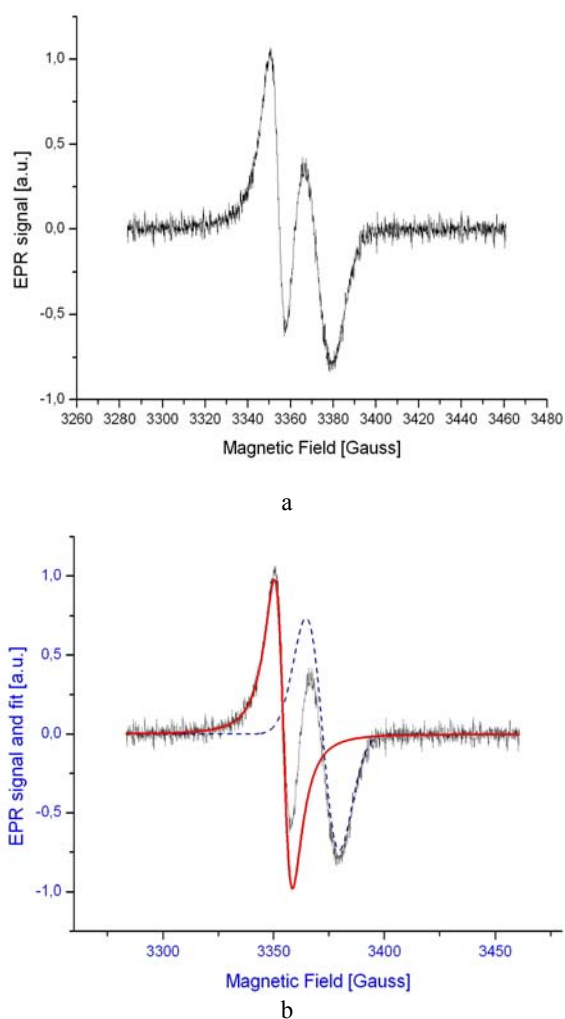


Fig. 2.a The EPR signal recorded on a  $\text{CaF}_2$  sample irradiated for 8 hours with 50 KeV X-ray photons. b The relative contributions of Lorentzian (F centers - thick, solid line) and of Gaussian (conduction electrons - thin, dotted line) lines changes from 85 % : 15 % to 55 % : 45 %.

Using the Poincaré fit method [8] we put in evidence the complexity of the EPR signal: a Lorentzian line (due to F centers) and Gaussian line (due to the conduction electrons) are superimposed. The measurements evidenced the increase of signal of the conduction electrons as one goes along the formation of the metal nano-structures in the crystalline structure of  $\text{CaF}_2$ . The  $\text{CaF}_2$  structure is initially insulating and without any magnetization. Once irradiated, the presence of EPR signal typical for F centers [1] supports our hypothesis concerning the role played by this type of defects in the formation of the nanometer metal inclusions. The experiments on doped samples allowed to refine our models.

## 2.2 Samarium-doped sample

In  $\text{CaF}_2$  the samarium ion (divalent or trivalent) substitutes the divalent cation  $\text{Ca}^{2+}$ .  $\text{Sm}^{2+}$  is not paramagnetic but poses a Van Vleck susceptibility. This susceptibility could produce, in certain neighborhood conditions, a shift of the EPR signal of  $\text{Sm}^{3+}$  centers.

### 2.2.1 Experiments on non-irradiated samples

The EPR spectra were recorded at 4 K for a fixed frequency (9.46 GHz) with a magnetic field varying between 7000 and 13000 Gauss. Our measurements show the presence of centers corresponding to two types of symmetry: ones with cubic and others with lower symmetry ( $C_{4v}$ ). In the last case the  $\hat{G}$  tensor corresponds to the axial symmetry of the axes [100], [010] or [001]. We obtained  $g_{\parallel} = 0.90 \pm 0.01$  and  $g_{\perp} = 0.77 \pm 0.01$ . The average value is  $\tilde{g} \approx 0.837$  along the direction  $\langle 100 \rangle$ . This value is higher than value for the isotropic  $g$ , corresponding to the cubic symmetry for  $\Gamma_7$  ( $g \approx 0.467$ ). This proves the existence of a magnetic exchange between  $\text{Sm}^{3+}$  and  $\text{Sm}^{2+}$ . The exchange provokes, also, a  $\Delta g$  shift.

The  $\text{Sm}^{3+}$  spectrum contains, for an arbitrary angle, three lines (Fig. 3).

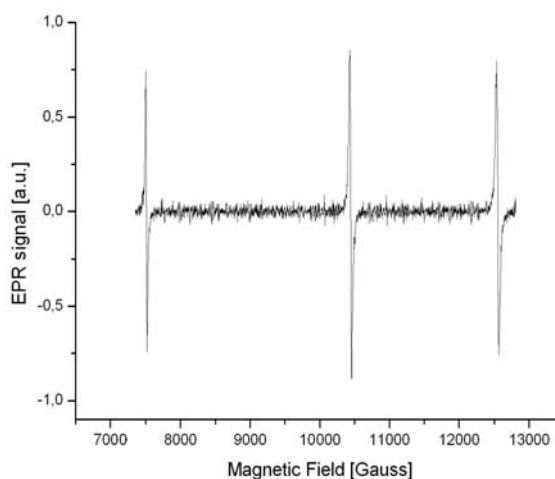


Fig. 3. EPR signal of  $\text{Sm}^{3+}$ :  $\text{CaF}_2$  irradiated 8 hours with 50 keV X photons.

For various orientations the values of  $g$  show an angular anisotropy. For an axial symmetry of the crystal field type  $\langle 100 \rangle$  there are, for an angle  $\theta$ , three classes of resonators, according to the three possibilities: [100], [010] and [001]. If  $\theta$  is the angle between [100] direction and the magnetic field  $\vec{H}_0$ , the angle  $\theta$  takes the values

$$\theta, \frac{\pi}{2} - \theta \text{ and } \frac{\pi}{2}$$

for the resonators x, y, z.

### 2.2.2 Experiments on irradiated samples

The irradiation with 50 keV X-rays leads to the formation of point defects. These defects favor a supplementary valence change  $\text{Sm}^{2+} \rightarrow \text{Sm}^{3+}$ . This change is produced by an extrinsic mechanism due to interstitial de-location of Sm or by the vicinity of a defect in the ligand lattice. The last possibility seems to be more probable, the formation of fluorine vacancies being the most probable process at this irradiation level. As a result of the irradiation, a global increase of  $\sim 10\%$  of the EPR signal due to the increase of the number of resonant centers. On the other hand, the line positions are shifted, as a result of the new numerical presence of the  $\text{Sm}^{2+}$  ions. The last effect is provoked by the modification (via the number  $p$  of the  $\text{Sm}^{2+}$  nearest neighbors) of the Van Vleck susceptibility. This suggests that approximately 10%  $\text{Sm}^{2+}$  ions became  $\text{Sm}^{3+}$ .

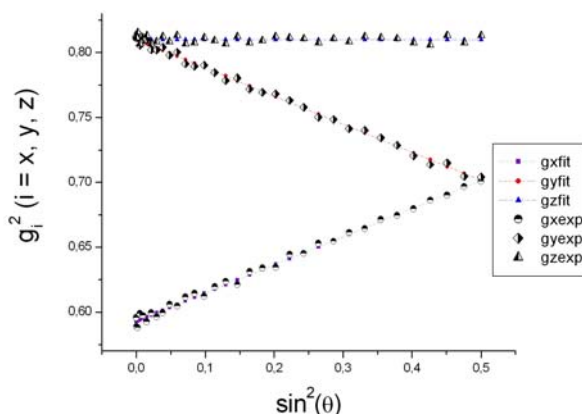


Fig. 4. Diagram  $[g^2; \sin^2 \theta]$  for  $\text{Sm}^{3+}: \text{CaF}_2$  irradiated 8 hours with 50 keV X photons.

In this case, the charge compensation plays a determinant role when the symmetry of the ligand field changes. The analysis of the EPR signals of  $\text{Sm}^{3+}$ , modified by the symmetry change of the sites, is a very difficult task. As we already mentioned, the gap between the ground state  ${}^6\text{H}_{5/2}$  and the first excited state  ${}^6\text{H}_{7/2}$  is rather small ( $\sim 1000 \text{ cm}^{-1}$ ). It is easier to interpret these symmetry changes for the EPR signals of  $\text{Er}^{3+}$  ions: the energy gap separating the ground state  ${}^4\text{I}_{15/2}$  and the first excited state  ${}^4\text{I}_{13/2}$  is much larger ( $\sim 6000 \text{ cm}^{-1}$ ).

### 2.3. Erbium-doped sample

The trivalent  $\text{Er}^{3+}$  ions enter the cubic structure of  $\text{CaF}_2$  by a heterovalent substitution of  $\text{Ca}^{2+}$ . The charge compensation induces the formation of a defect which modifies the site symmetry. Three types of symmetry are evidenced: cubic, tetragonal and / or trigonal. In tetragonal symmetry there are three equivalent sites along the  $[100]$ ,

$[010]$  and  $[001]$  crystal axes. The proposed notations for  $[100]$ ,  $[010]$  and  $[001]$  crystal axes are:  $T_x$ ,  $T_y$  and  $T_z$ . The four trigonal axes correspond to the directions  $[111]$ ,  $[\bar{1}11]$ ,  $[\bar{1}\bar{1}1]$  and  $[1\bar{1}\bar{1}]$ .

#### 2.3.1 Experiments on non-irradiated samples

The EPR spectra were recorded at 4 K and 9.46 GHz. The magnetic field varies around 1000 Gauss. The diagram  $[g^2 / \sin^2 \theta]$  gives the components of the  $\hat{G}$  tensor. The results are given in Table 1.

Table 1. Components of the  $\hat{G}$  tensor in non-irradiated  $\text{Er}^{3+}: \text{CaF}_2$ .

Components of the $\hat{G}$ tensor $\rightarrow$ Symmetry $\downarrow$	$g_{\parallel}$	$g_{\perp}$
Cubic	6.80	6.80
Tetragonal	7.80	6.25
Trigonal	3.30	8.55

The obtained values are close to the values reported by Ranon and Low [7] for the tetragonal spectrum of the type I, i. e.  $g_{\parallel} = 7.78$  and  $g_{\perp} = 8.54$  (Fig. 5), but we found very different intensities, corresponding to the same angular values of the magnetic field relative to the  $T_z$  axis. For the non-irradiated sample we found that the

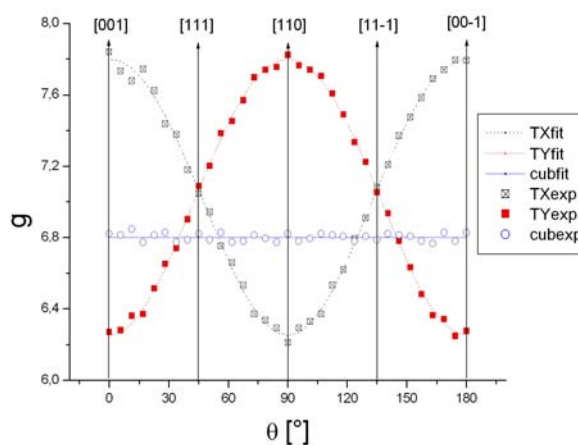


Fig. 5. Angular dependence of the components of the  $\hat{G}$  tensor in non-irradiated  $\text{Er}^{3+}: \text{CaF}_2$ ;  $\theta$  is the angle between  $[100]$  direction and the magnetic field  $\vec{H}_0$ .

intensities of the signals are in the following ratios: T (tetragonal) : t (trigonal) : c (cubic) = 4 : 2 : 3. No tetragonal or trigonal signal of the type II (cited in [7]) was detected in our spectra.

### 2.3.2 Experiments on irradiated samples

For the irradiated samples the lines have the angular evolution given in Fig. 6. The angular diagrams were constructed from the EPR spectra whose parameters were identified using the Poincaré's treatment [8].

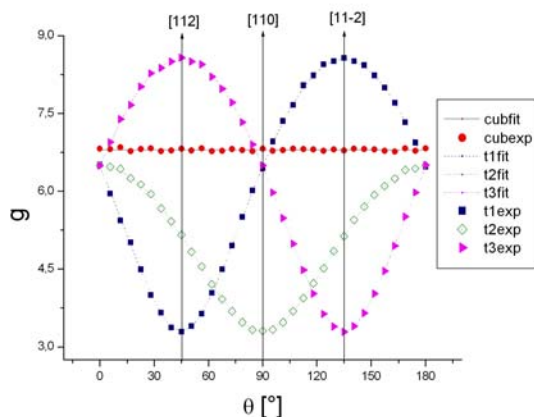


Fig. 6. Angular dependence of the components of the  $\hat{G}$  tensor in  $Er^{3+}: CaF_2$  irradiated 8 hours with 50 keV X photons.

In this case, the intensity ratio is  $T : t : c = 8 : 5 : 4$ . We must emphasize that our crystals were grown in neutral atmosphere. The significant increases of the trigonal signal in the irradiated samples are probably due to the presence of oxygen. We suppose that the absence of the trigonal spectra of type II (whose intensity increase is reported in [7]) is related to compensation with oxygen placed diagonally in a fluorine position. This oxygen came from the  $Er_2O_3$  doping.

### 3. Conclusion

The comparison of  $Er^{3+}$  EPR spectra in irradiated and in non-irradiated  $CaF_2$  samples led us to the following conclusions:

- the lines conserve their angular dependence;
- the intensity of the cubic lines decreases;
- the intensity of the tetragonal lines increases slightly;
- the intensity of the trigonal lines shows a significant increase;
- the total number of resonant  $Er^{3+}$  centers is rigorously the same in both irradiated and non-irradiated samples.

We put in evidence a symmetry change of the ligands  $F^-$  from cubic toward  $C_{4v}$ . The tetragonal change is explained as a result of charge compensation with an interstitial defect created by an  $F^-$  ion occupying the center of the neighbor ligands, initially empty. In the trigonal case we suggest that an  $O^{2-}$  ion replaces a  $F^-$  ion in a cube corner of neighboring fluorine ions.

### References

- [1] F. Beuneu, C. Florea, P. Vajda – Radiation Effects and Defects in Solids, **136**, 175, (1995).
- [2] Ch. T. de Montpreville – Note Technique SRPM – CEA (1985).
- [3] E. Johnson, L. Chaderton – Radiation Effects and Defects in Solids, **79**, 183 (1983).
- [4] A. Hughes, S. Jain – Adv. in Phys., **28**, 717 (1979).
- [5] Y. Quéré – Points Defects in Solids, Masson Ed. Paris (1967).
- [6] Ch. H. de Novion – Note Technique SESI – CEA (1993).
- [7] U. Ranon, W. Low – Phys. Rev. **132** 1609, (1963).
- [8] C. Florea – Note Technique SESI – CEA (1994).

\*Corresponding author: c.florea@esiee.fr